Spatial Distributions of Thin Oxide Charging in Reactive Ion Etcher and MERIE Etcher

Hyungcheol Shin, Ko Noguchi, Xue-Yu Qian, Neeta Jha, *Member, IEEE,* Graham Hills, and Chenming Hu, *Fellow, IEEE*

***Abstract*—The spatial variation of the oxide charging across a wafer in a magnetically enhanced reactive ion etcher (MERIE) was investigated and compared with that in a reactive ion etcher (RIE). The polarity as well as the magnitude of the oxide charging current were determined by evaluating quasi-static *CV* curves for MOS capacitors. In a MERIE etcher with a static magnetic field, oxide charging is negative for about half of the wafer and positive for the other half of the wafer. A model is proposed to explain how lateral magnetic field affects the spatial distribution of charging across the wafer in a MERIE etcher.**

I. Introduction

PLASMA etching is widely used in the fabrication of VLSI's to realize fine-line patterning. However, damage to processed structures has been observed and attributed to charging of the oxide during plasma exposure [1]–[13]. Magnetized plasma etchers such as magnetically enhanced reactive ion etch (MERIE) reactors or ECR etchers have been introduced as alternatives to conventional reactive ion etchers (RIE's). They produce higher ion densities at lower energy. A better knowledge of oxide damage produced by these etchers is needed [9]–[13].

In this paper, thin oxide stressing by a MERIE etcher and by an RIE etcher was investigated to understand how magnetic field affects the charging to devices. The distributions of oxide charging current across the wafer in the two etcher configurations are compared.

II. Experiment

The test structures are MOS capacitors with 11.8-nm gate oxide. The thin oxide area of test capacitors is 40 000 μm^2. The Al pattern is 80 000 μm^2 in area and 6820 μm in edge length. Aluminum etching with patterned photoresist on top of aluminum layer was done both in a RIE etcher and a MERIE etcher. Both systems were powered by a 13.56-MHz RF generator. Reactive ion etching was done in a parallel plate etcher at 250 W. Photoresist was stripped by wet process before testing. There was no temperature cycling after aluminum etching. Normally, a magnetic field in a MERIE etcher rotates to obtain better etch rate uniformity. In this experiment, the magnetic field was either rotated at the normal 0.5 Hz or stationary. The rotating magnetic flux density was a normal 50 G. In addition, a high static magnetic flux density of 140 G was used to exaggerate the oxide damage. Control wafers were also fabricated by wet etching.

Manuscript received September 14, 1992; revised December 4, 1992. This work was supported by the Semiconductor Research Corporation, Sandia Laboratory, Signetics, Texas Instruments, Rockwell International, and AMD under the MICRO program and ISTO/SDIO administered by ONR under Contract N00014-85-K-0603.

H. Shin and C. Hu are with the Department of Electrical Engineering and Computer Sciences and the Electronics Research Laboratory, University of California, Berkeley, CA 94720.

K. Noguchi is with the Department of Electrical Engineering and Computer Sciences and the Electronics Research Laboratory, University of California, Berkeley, CA 94720 on leave from NEC Corporation, Kanagawa, Japan.

X.-Y. Qian, N. Jha, and G. Hills are with Applied Materials, Applied CVD and Etch Technologies (ACET), Santa Clara, CA 95054.

IEEE Log Number 9207083.

III. Results and Discussions

Fig. 1 compares the oxide charging current distribution in a MERIE system with normal rotating field as well as that in an RIE etcher with identical etching rates. The charging current was extracted by comparing *CV* characteristics after plasma etching with those after wet etching and subsequent electrical stress [7]. The order of magnitude of the charging current can also be calculated from plasma parameters [8]. For RIE etching, the wafer center received more-charging than the wafer edge because the etcher has higher plasma intensity and higher etch rate in the wafer center [8]. Such spatial patterns cannot be easily determined from oxide breakdown data which are often more complicated to interpret because of the random distribution of oxide defects. For the reactors used in this experiment, the charging in the MERIE etcher is less than the RIE etcher except for wafer edge and it's more uniform in the MERIE etcher. Also note that the charging is smallest at the wafer center and increases toward the wafer edge.

To investigate the charging distribution in a MERIE etcher, Al was etched with a large static magnetic field. Fig. 2 shows quasi-static *CV* characteristics at two different locations on the wafer (X and Y) after static-field magnetron etching. *CV*'s of capacitors in region Y showed negative flat-band voltage shift (ΔV_{FB}). On the other hand, *CV*'s of capacitors in region X showed only distortion and a negligible ΔV_{FB}. It has been known that *CV* characteristics after negative gate current stressing show a

0741-3106/93$03.00 © 1993 IEEE

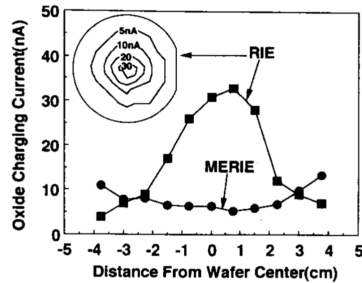

Fig. 1. Oxide charging current distribution across the wafer in a MERIE system with rotating field as well as that in an RIE etcher. The radial distribution of oxide charging across the wafer for RIE etching is shown inside the figure. A rotating magnetic field of 50 G was used during MERIE etching.

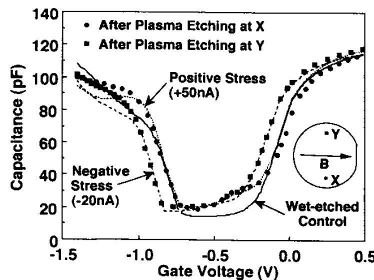

Fig. 2. Quasi-static CV's after a constant current stress for both polarities. The CV's at the location X (solid circle) and Y (solid square) after plasma etching match very well with CV's of wet-etched samples after +50-nA stress (dotted line) and −20-nA stress (broken lines), respectively. There is a negative flat-band voltage shift after negative stressing but not after positive stressing. CV of a wet-etched control capacitor is also shown for comparison.

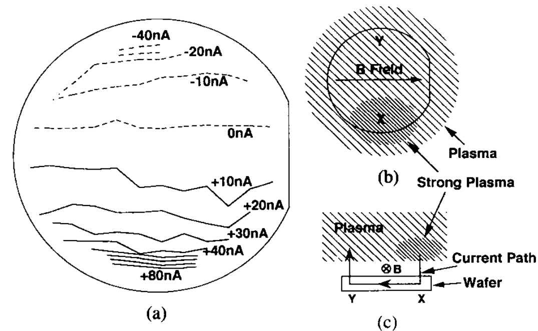

Fig. 3. (a) Charging current distribution across the wafer during static-field MERIE etching. The magnetic field was set at an extreme value of 140 G. About half of the wafer received a positive charging and the other half received a negative charging during etching. (b) Dark region (side X) indicates strong plasma. (c) Plasma charging current path is shown schematically.

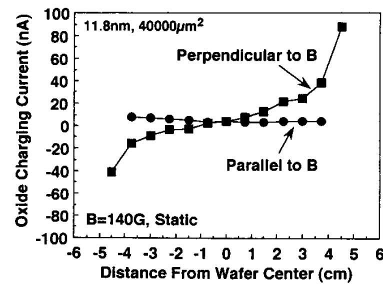

Fig. 4. Oxide charging current for two directions across the wafer, parallel and perpendicular to the magnetic field, for the static-field MERIE exposure.

negative ΔV_{FB} in addition to distortion due to preferential hole trapping near the anode, i.e., the silicon–oxide interface [14]. After positive stressing, ΔV_{FB} is negligible and only distortion is observed. This was confirmed by electrical stressing (two broken curves in Fig. 2). The conclusion is that capacitors in region Y received a negative gate-current charging during etching, whereas the capacitors in region X received a positive current charging.

To further confirm the charging polarity, a series of short-duration low-voltage pulses were applied to capacitors after MERIE etching as well as to capacitors after electrical stressing to detrap the holes from the oxide–silicon interface [15]. The detrapping (CV shift) behavior led to the same conclusion.

Fig. 3(a) shows contours of the extracted oxide charging current across the wafer in a static-field MERIE reactor. About half of the wafer collected positive current while the other half collected negative current. Similar distributions were obtained by using EEPROM [12] or MNOS [13]. The charging current along two directions, parallel and perpendicular to the magnetic field, are plotted in Fig. 4.

Due to the static magnetic field perpendicular to the electric field inside the sheath region, secondary electrons emitted from the wafer surface drift with a cycloid motion toward one side of the wafer (side X in Fig. 3(b)), enhancing the ionization process and increasing the plasma density above region X. In fact, a more intense glow was observed in region X than region Y. Since electron mobility is much higher than ion mobility, there is a net electron flow in the X to Y direction inside plasma. Local currents are balanced by electrons flowing from plasma through the oxide in region Y into the wafer and exit through oxide in region X to neutralize the net ion flow toward the wafer there (Fig. 3(c)).

When the magnetic field rotates, more charging occurs around the wafer edge (Fig. 1) since the charging current for static field case is very small in the wafer center band (Fig. 3(a)).

IV. Summary

The charging currents experienced by MOS capacitors during plasma etching is characterized for a MERIE reactor and compared with that for an RIE etcher. The polarity as well as the magnitude of the charging current were determined from quasi-static CV characteristics. A static-field MERIE system generates a charging current of opposite polarities in the two halves of the wafer with zero current near the middle due to the electron drift by

Lorentz force. Upon rotating the magnetic field, a low damage region exists in the center of the wafer.

REFERENCES

[1] C. Gabriel and J. C. Mitchener, "Reduced device damage using an ozone based photoresist removal process," *Proc. SPIE*, vol. 1086, pp. 598–603, 1989.

[2] F. Shone *et al.*, "Gate oxide charging and its elimination for metal antenna capacitor and transistor in VLSI CMOS double layer metal technology," in *Symp. VLSI Tech. Dig. Papers*, 1989, pp. 73–74.

[3] Y. Kawamoto, "MOS gate insulator breakdown caused by exposure to plasma," in *Proc.* 1985 *Dry Process Symp., Inst. Elect. Eng. Japan*, Oct. 1985, pp. 132–137.

[4] K. Tsunokuni, K. Nojiri, S. Kuboshima, and K. Hirobe, "The effect of charge buildup on gate oxide breakdown during dry etching," in *Extended Abstr. 19th Conf. Solid State devices Mater.*, 1987, pp. 195–198.

[5] I.-W. Wu, R. H. Bruce, G. B. Anderson, M. Koyanagi, and T. Y. Huang, "Damage to gate oxides in reactive ion etching," *Proc. SPIE*, vol. 1185, pp. 284–295, 1989.

[6] S. Fang and J. McVittie, "Thin-oxide damage from gate charging during plasma processing," *IEEE Electron Device Lett.*, vol. 13, no. 5, pp. 288–290, May 1992.

[7] H. Shin, C.-C. King, T. Horiuchi, and C. Hu, "Thin oxide charging current during plasma etching of aluminum," *IEEE Electron Device Lett.*, vol. 12, no. 8, pp. 404–406, Aug. 1991.

[8] H. Shin, C.-C. King, and C. Hu, "Thin oxide damage by plasma etching and ashing processes," in *Proc. IEEE IRPS*, 1992, pp. 37–41.

[9] S. Fang and J. McVittie, "A model and experiments for thin oxide damage from wafer charging in magnetron plasmas," *IEEE Electron Device Lett.*, vol. 13, no. 6, pp. 347–349, June 1992.

[10] M. Sekine *et al.*, "Gate oxide breakdown phenomena in magnetized plasma," in *Proc. Dry Process Symp.*, 1991, pp. 99–103.

[11] W. Greene, J. Kruger, and G. Kooi, "Magnetron etching of polysilicon: Electrical damage," *J. Vac. Sci. Technol.*, pp. 366–369, 1991.

[12] T. Namura *et al.*, "Wafer charging in different types of plasma etchers," *Proc. SPIE*, vol. 1593, pp. 11–22, Sept. 1991.

[13] T. Namura, H. Okada, Y. Naitoh, Y. Todokoro, and M. Inoue, "Charge buildup in magnetized process plasma," *Japan. J. Appl. Phys.*, vol. 30, no. 7, pp. 1576–1580, July 1991.

[14] D. Dumin, K. Dickerson, M. Hall, W. Vigrass, and G. Brown, "Correlation of wearout and breakdown in sub-10 nm silicon oxide," in *IEDM Tech. Dig.*, 1988, pp. 718–721.

[15] V. Lakshmanna and A. Vengurlekar, "Logarithmic detrapping response for holes injected into SiO2 and the influence of thermal activation and electric fields," *J. Appl. Phys.*, vol. 63, no. 9, pp. 4548–4554, May 1988.